JGR-Atmospheres

Supporting Information for

Regulation of synoptic circulation in regional $PM_{2.5}$ transport for heavy air pollution: study of 5-year observation over central China

Weiyang Hu[1], Tianliang Zhao[1], Yongqing Bai[2], Shaofei Kong[3], Lijuan Shen[1], Jie Xiong[2], Yue Zhou[2], Yao Gu[1], Junnan Shi[4], Huang Zheng[3], and Xiaoyun Sun[1]

[1]Climate and Weather Disasters Collaborative Innovation Center, Key Laboratory for Aerosol-Cloud-Precipitation of China Meteorological Administration, PREMIC, Nanjing University of Information Science &Technology, Nanjing, 210044, China.

[2]Institute of Heavy Rain, China Meteorological Administration, Wuhan, 430205, China.

[3]Department of Atmospheric Sciences, School of Environmental Studies, China University of Geosciences (Wuhan), Wuhan, 430074, China.

[4]Taishan meteorological station of Shandong province, Taishan, 271000, China

Correspondence: tlzhao@nuist.edu.cn (T.L. Zhao) and 2007byq@163.com

Contents of this file

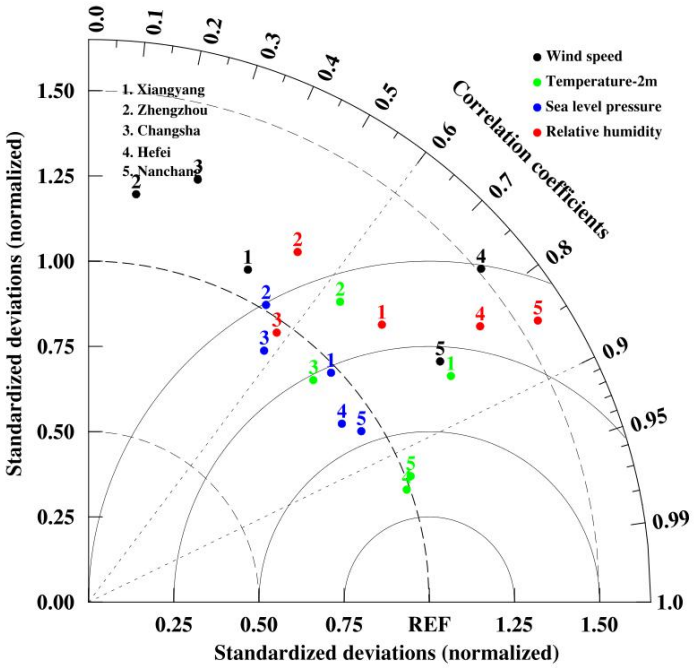

Figure S1. Comparisons in Taylor plots (Taylor, 2001) manifesting the standard deviations and correlation coefficients between the simulated and observed meteorological elements including 10-m wind speed, 2-m air temperature, air pressure and relative humidity at 5 urban sites (Xiangyang, Zhengzhou, Changsha, Hefei, and Nanchang) over the THB.

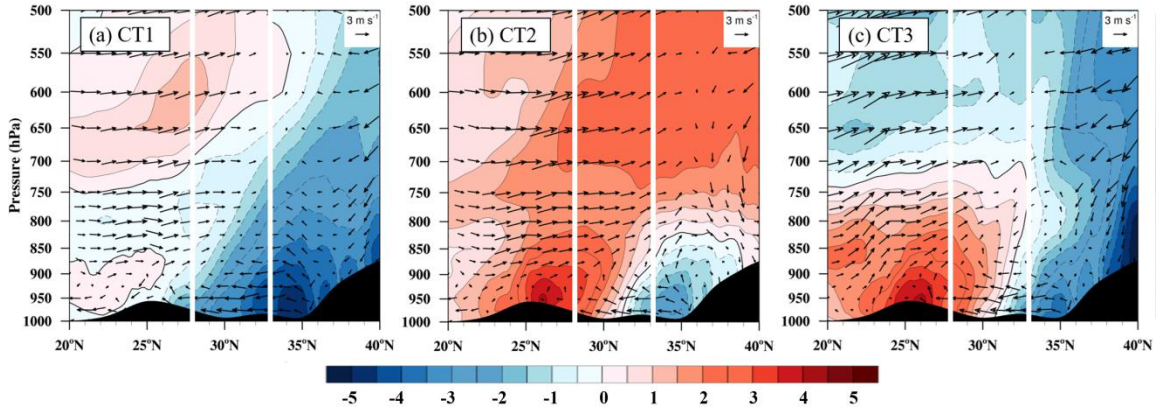

Figure S2. Vertical cross sections of air temperature anomalies (color contours, ℃) and wind vectors for three synoptic circulation types (a) CT1, (b) CT2, (c) CT3 over CEC. The vertical wind components were multiplied by 20 to better display vertical circulations. With the white frames marking atmospheric columns over the THB in central China.

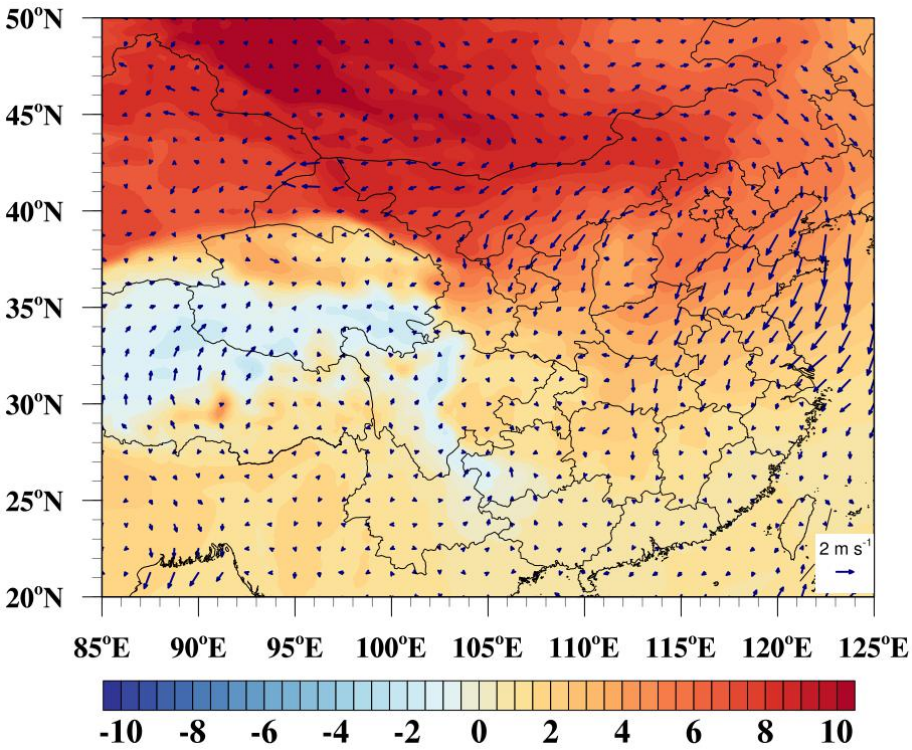

Figure S3. Distribution of anomalies of sea level pressure (unit: hPa) and 10-m wind vectors (unit: m s $^{-1}$) in CT1 relatively to the wintertime averages over 2015–2019.

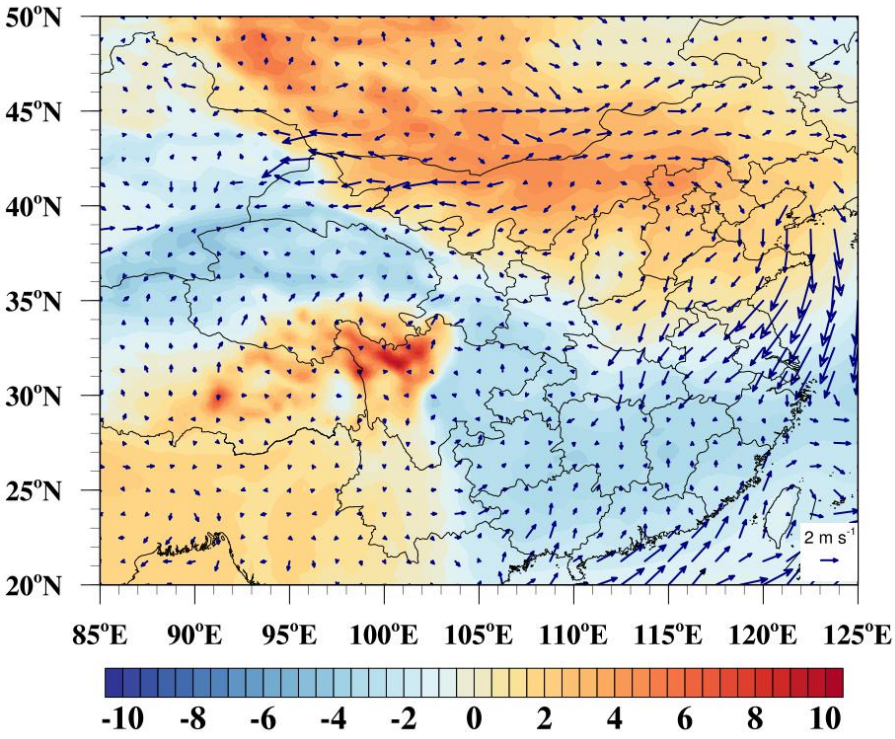

Figure S4. Distribution of anomalies of sea level pressure (unit: hPa) and 10-m wind vectors (unit: m s $^{-1}$) in CT3 relatively to the wintertime averages over 2015–2019.

Table S1 WRF model configurations.

Regions	CEC
Domain size	265 × 541 grid cells; 200 × 283 grid cells
Horizontal resolution	30 km; 10 km
Vertical resolution	33 sigma levels
Microphysics	Lin scheme
Longwave radiation	RRTM scheme
Shortwave radiation	Goddard shortwave scheme
Surface layer	MM5 similarity surface layer
Land-surface	the unified Noah land surface model
Urban canopy model	Single-layer UCM scheme
Boundary layer	YSU boundary layer scheme
Cumulus	Grell 3-D ensemble scheme

Photolysis	Fast-J
Spin-up time	48 h
Simulation period	Wintertime over 2015 to 2019

Table S2 Statistics of heavy air pollution days over the THB during 2015–2019.

Date (YYYYMMDD)	Number of cities with heavy air pollution	Average $PM_{2.5}$ concentrations ($\mu g\ m^{-3}$)	Maximum $PM_{2.5}$ concentrations ($\mu g\ m^{-3}$)
20151211	9	156	277
20151212	11	179	264
20151223	5	133	190
20151224	3	115	178
20151225	9	164	281
20151230	4	128	169
20160102	4	131	206
20160104	8	163	342
20160105	4	129	229
20160111	6	133	215
20160118	8	154	235
20160130	3	99	208
20160208	12	196	312
20160306	3	99	183
20161115	4	114	261
20161209	3	122	176
20161220	4	125	417
20170102	7	138	185
20170103	8	154	213
20170104	13	179	229
20170128	14	221	449
20170217	4	130	165
20170306	6	139	216
20170307	6	137	203
20171204	4	124	278
20171205	6	141	185
20171229	3	119	279
20171230	3	118	170
20180102	3	104	207
20180119	10	171	307

20180120	5	126	228
20180216	5	133	190
20181130	7	150	237
20181201	10	176	269
20181202	5	129	203
20190105	7	154	279
20190106	12	175	324
20190107	8	159	287
20190108	8	152	270
20190126	5	125	190
20190128	3	119	154
20190129	3	120	186
20190130	4	113	194
20190205	10	158	252
20191214	4	132	187
20191215	4	122	211

Table S3 Statistics of 30-day HPEs dominated by regional $PM_{2.5}$ transport with corresponding transport contribution rates to the THB' s regional $PM_{2.5}$ concentrations.

ID	Date (YYYYMMDD)	Contribution rates (%)
1	20151211	66.90
2	20151212	70.90
3	20151223	70.60
4	20151224	70.30
5	20160104	75.00
6	20160105	80.30
7	20160111	63.20
8	20160118	73.70
9	20160130	78.90
10	20161115	75.00
11	20161209	40.70
12	20161220	60.90
13	20170103	44.70
14	20170217	62.20
15	20170306	61.50
16	20170307	53.40
17	20171204	69.70
18	20171205	56.40
19	20171229	30.10
20	20181130	50.00

21	20190105	76.80
22	20190106	45.60
23	20190107	36.60
24	20190108	77.60
25	20190126	84.90
26	20190128	50.00
27	20190129	59.80
28	20190130	28.90
29	20191214	38.30
30	20191215	52.40
average	-	60.20

Table S4 Statistics of three types of synoptic circulation with the date (YearMonthDay) during wintertime over 2015–2019, and CT indicated by the numbers 1, 2 or 3 respectively for three synoptic circulation types CT1, CT2 or CT3.

Date (YYYYMMDD)	CT	Date (YYYYMMDD)	CT
20151211	2	20170307	1
20151212	2	20171204	1
20151223	1	20171205	1
20151224	2	20171229	1
20160104	3	20181130	2
20160105	3	20190105	1
20160111	1	20190106	1
20160118	3	20190107	1
20160130	1	20190108	2
20161115	3	20190126	1
20161209	2	20190128	1
20161220	1	20190129	2
20170103	2	20190130	2
20170217	2	20191214	2
20170306	1	20191215	2

Table S5 Regional averages of meteorological variables 2-m air temperature (T), relative humidity (RH), air pressure (P) and 10-m wind speed (WS) as well as $PM_{2.5}$ concentrations over the THB under three synoptic circulation types CT1, CT2 and CT3.

Synoptic types	T (°C)	RH (%)	P (hPa)	WS (m s^{-1})	$PM_{2.5}$ (μg m^{-3})
CT1	5.2	77.5	1027.6	2.6	143.5

CT2	7.4	77.9	1025.5	2.7	154.9
CT3	5.6	83.3	1024.6	3.1	152.6

Reference

Taylor, K. E. (2001). Summarizing multiple aspects of model performance in a single diagram. *Journal of Geophysical Research-Atmosphere*, *106*, 7183 – 7192. doi: 10.1029/2000JD900719